Physiol Genomics 35: 341–350, 2008.
First published September 23, 2008; doi:10.1152/physiolgenomics.90255.2008.

Hypothalamus transcriptome profile suggests an anorexia-cachexia syndrome in the *anx/anx* mouse model

Josep Maria Mercader,[1,2] Juan José Lozano,[3,4] Lauro Sumoy,[3] Mara Dierssen,[1,5] Joana Visa,[6] Mònica Gratacòs,[1,2] and Xavier Estivill[1,2,7]

[1]*Genes and Disease Program, Center for Genomic Regulation (CRG-UPF);* [2]*CIBER en Epidemiología y Salud Pública (CIBERESP),* [3]*Bioinformatics and Genomics Program, CRG-UPF;* [4]*CIBER de Enfermedades Hepáticas y Digestivas (CIBEREHD);* [5]*CIBER de Enfermedades Raras (CIBERER);* [6]*Servei Estabulari, IDIBELL, L'Hospitalet de Llobregat; and* [7]*Experimental and Health Sciences Department, Pompeu Fabra University, Barcelona, Catalonia, Spain*

Submitted 20 May 2008; accepted in final form 18 September 2008

Mercader JM, Lozano JJ, Sumoy L, Dierssen M, Visa J, Gratacòs M, Estivill X. Hypothalamus transcriptome profile suggests an anorexia-cachexia syndrome in the *anx/anx* mouse model. *Physiol Genomics* 35: 341–350, 2008. First published September 23, 2008; doi:10.1152/physiolgenomics.90255.2008.—The *anx/anx* mouse displays poor appetite and lean appearance and is considered a good model for the study of anorexia nervosa. To identify new genes involved in feeding behavior and body weight regulation we performed an expression profiling in the hypothalamus of the *anx/anx* mice. Using commercial microarrays we detected 156 differentially expressed genes and validated 92 of those using TaqMan low-density arrays. The expression of a set of 87 candidate genes selected based on literature evidences was also quantified by TaqMan low-density arrays. Our results showed enrichment in deregulated genes involved in cell death, cell morphology, and cancer, as well as an alteration of several signaling circuits involved in energy balance including neuropeptide Y and melanocortin signaling. The expression profile along with the phenotype led us to conclude that *anx/anx* mice resemble the anorexia-cachexia syndrome typically observed in cancer, infection with human immunodeficiency virus or chronic diseases, rather than starvation, and that *anx/anx* mice could be considered a good model for the treatment and investigation of this condition.

feeding regulation; chronic disorders; gene expression; TaqMan low-density arrays; microarrays

ENERGY BALANCE AND BODY WEIGHT regulation are major homeostatic processes, and the disruption of their regulatory mechanisms can cause several complications, leading to death in the worst cases. In humans, deregulation of these mechanisms occurs in patients with eating disorders (ED), such as anorexia nervosa (AN) and bulimia nervosa (BN), and obesity. ED and obesity, major health problems in adolescents, are associated with elevated risk for a broad range of physical and mental disorders during early adulthood (1, 6, 69). In developed countries, the incidence of AN or BN has dramatically increased in recent years (39), though other diseases such as cancer or chronic infections can be also associated with an energy balance impairment characterized by progressive weight loss and depletion of adipose and skeletal muscle reserves, known as cachexia, which can aggravate the outcome of the disease (73). In these cases, anorexia appears in response to acute and chronic infections, inflammation, and trauma, followed by severe loss of body weight due to a deregulation of the appetite-regulating hypothalamic circuitry.

One animal model proposed for the study of anorexia is the *anx/anx* mouse, a mutant that harbors a recessive mutation in chromosome 2, not yet identified, close to the *Pallidin* gene (36, 49). These mice display poor appetite resulting in growth failure and emaciated appearance, accompanied by abnormal behavior and neurological symptoms including body tremors, head weaving, hyperactivity, and uncoordinated gate (49). At the biochemical level, these mice show a reduced expression of several neuropeptides, such as pro-opiomelanocortin (POMC), neuropeptide Y (NPY) (12), and cocaine amphetamine-related transcripts in the arcuate nucleus (35), as well as a general hyperserotonergic activity and altered dopamine signaling in the striatum (33, 37, 70).

To our knowledge, the only available expression profile study performed in the *anx/anx* model found a deregulation of the orexigenic NPY/AGRP system and an upregulation of different sets of genes of the immune/inflammatory response in the hypothalamus (44). The authors pointed to a relationship between the inflammatory process revealed by the expression profile and the anorexic phenotype observed in these mice.

However, although many genes identified in the oligonucleotide array were also confirmed through the hybridization of a cDNA microarray, the study validated the differential expression of few genes with a real-time PCR alternative method, and much biological information, especially concerning genes with a mild effect, might still not be untangled.

To obtain a greater understanding of the pathogenetic mechanisms involved in the anorexic phenotype of *anx/anx* mice, we profiled its transcriptome in the hypothalamus, a critical brain area involved in the chemical encoding of feeding behavior. For that purpose we used oligonucleotide DNA microarrays to screen ~44,000 probes and further performed an extensive post hoc validation of 92 differentially expressed genes by real-time quantitative RT-PCR low-density arrays (TaqMan). We also included 87 additional assays of candidate genes involved in obesity, eating behavior, and ED selected from literature searches.

Address for reprint requests and other correspondence: X. Estivill, Genes and Disease Program, Center for Genomic Regulation (CRG), Plaça Charles Darwin s/n (Dr. Aiguader 88), PRBB Bldg., Rm. 521, 08003 Barcelona, Catalunya, Spain (e-mail: xavier.estivill@crg.es); and M. Gratacòs, CIBER en Epidemiología y Salud Pública (CIBERESP), Genes and Disease Program, Center for Genomic Regulation (CRG), Plaça Charles Darwin s/n (Dr. Aiguader 88), PRBB Bldg., Rm. 521, 08003 Barcelona, CATALUNYA, Spain (e-mail: monica.gratacos@crg.es).

The costs of publication of this article were defrayed in part by the payment of page charges. The article must therefore be hereby marked "*advertisement*" in accordance with 18 U.S.C. Section 1734 solely to indicate this fact.

MATERIALS AND METHODS

Animals, Tissue Dissection, and Sex Genotyping

Homozygous *anx/anx* mice were produced from heterozygous breeder pairs (B6C3Fe a/a-anx/J) obtained from the Jackson Laboratory. Postnatal *day 16* weanling mice housed with their parents were separated into two groups: *anx/anx* and control mice. *anx/anx* mice were identified by their reduced body weight, body tremor, and mild hyperactivity. Because homozygous and heterozygous mice cannot be phenotypically nor genotypically distinguished from wild types (wt), control groups probably contained both genotypes (wt/wt or wt/anx). *anx/anx* and control mice were allowed ad libitum access to the mother, food, and water. Three *anx/anx* and three control mice were anesthetized with 3% isoflurane and decapitated, and the hypothalamus was dissected. Tissues were immediately frozen with liquid nitrogen and stored until the experiments were performed. RNA was extracted from the tissue using TRIzol (Invitrogen), following manufacturer's recommendations. All RNAs used had RNA integrity numbers ranging between 8.4 and 8.9 and 28S/18S ratios between 1.3 and 1.6. *anx/anx* animals are quite smaller than their control littermates, and sex phenotyping might be confusing in some cases. As there might be differential expression due to sex differences, we rechecked the sex through a PCR as described by Clapcote and Roder (18) on DNA extracted from tail biopsies by previously described methods (46). All experimental procedures were approved by the local ethical committee (CEEA-IMIM and CEEA-PRBB) and met the guidelines of local (Spanish law 32/2007 and Catalan law 5/1995) and European regulations (EU directive no. 86/609, EU decree 2001-486), and the Standards for Use of Laboratory Animals no. A5388-01 (National Institutes of Health). The Center for Genomic Regulation (CRG) is authorized to work with genetically modified organisms (A/ES/05/I-13 and A/ES/05/14). Researchers had a specific qualification for experimentation on live animals.

Microarray Hybridization

Microarray expression profiles were obtained using the 44K Whole Mouse Genome (ref. G4122A) oligonucleotide platform (Agilent Technologies, Palo Alto, CA), and the RNA labeling and hybridization process was performed following the manufacturer's instructions. We used three replica groups consisting of three pairs of samples: for each pair, one *anx/anx* mouse was compared with a control mouse from the same litter. Moreover, and to avoid bias labeling artifacts, dye swap experiments were performed for two of the *anx/anx*-control pairs, resulting in a total of five arrays. Dye swap experiments were performed to avoid a bias toward genes that are differentially hybridized when labeled to a particular dye. Fluorescent images were obtained with an Agilent G2565BA scanner. Microarray images were quantified using GenePix 6.0 (Axon) software. Only spots with signal intensities twice above the local background, not saturated, and not flagged by GenePix were considered reliable and used for subsequent analysis. Extracted intensities were subtracted from the local background, and the log2 ratios were normalized in an intensity-dependent fashion by global LOWESS. Target genes were considered as differentially expressed when <0.001 false discovery rate (FDR), using significant analysis of microarrays (SAM) test implemented in R (75). All quantitative and statistical analyses were performed using the Limma package in the R environment (68).

Following the MIAME standard for microarray data, the expression data reported in this paper have been deposited in the Gene Expression Omnibus (GEO) (http://www.ncbi.nlm.nih.gov/geo) database (series GSE11426).

TaqMan Low-density Arrays

Selection of ABI assays. We selected 92 differentially expressed genes <0.001 FDR (0.1%), corresponding to 92 "made to order" assays, the ones available to perform TaqMan low-density arrays (TLDA), through the ABI web server (www.applied.biosystems.com). Assays for 87 additional candidate genes were also selected from several web resources, literature collection, and data obtained from our laboratory. In total, we selected 176 nonredundant assays, as three of them, for genes *Ppargc1a*, *Gabra2,* and *Gad2*, were selected based on both 0.001 FDR and literature search. We selected 15 additional putative housekeeping genes to search for the less variable endogenous controls to use as normalization factors. Supplementary Table S2[1] summarizes all the selected ABI assays and their criteria used for selection.

For the qPCR experiments, the same RNAs used for the microarray experiments were used. For three *anx/anx* mice and three control mice (thus three biological replicates) we performed two technical replicates, resulting in a total of 12 TLDA plates. cDNA was obtained using the cDNA with High Capacity Archive Kit from Applied Biosystems (Foster City, CA). To avoid genomic DNA contamination, RNA was treated with DNase I (2 U/μl; Ambion, Applied Biosystems) at 37°C for 30 min followed by inactivation with DNase inactivation reagent (Ambion, Applied Biosystems). cDNA was obtained using the cDNA with High Capacity Archive Kit from Applied Biosystems. DNA contamination was discarded through the amplification of an exon junction fragment of ubiquitin-like 4 (Ubl4) using the following primers: 5′-GGCAGCTGATCTC-CAAAGTCCTGG-3′ and 5′-AAC-GTTCGATGTCATCCAGT-GTTA-3′. This results in a higher-size DNA band in an agarose gel when DNA contamination is present. PCR master mix, prepared with TaqMan Universal PCR Master mix and cDNA, was loaded to TLDA card and run in a 9700 HT Applied Biosystems Real Time PCR machine following manufacturer's instructions (Applied Biosystems).

TaqMan Data Analysis

Real-time amplification curves and Ct values were calculated using SDS software version 2.1.1 software (Applied Biosystems). For each cDNA sample, two replicate TLDA assays were performed. To calculate the relative quantities for each sample, we used qbase software (28). We tried two methods to calculate the relative ΔCT values: the classical method normalizing the expression by a single endogenous control, and normalizing for the three most stable genes (less variable across conditions) using *GeNorm* software v3.4 (76). Log2 linear regression analysis was performed to assess how well real-time PCR using TLDA correlated with microarray Agilent results. R^2 and coefficients, including the *b* constant, were calculated using the classical method, normalizing by a single endogenous control, β-actin, or normalizing by the geometric mean of the three most stable genes selected using *GeNorm*. When plotting all the genes, we did not observe many differences between the R^2 coefficients using the two methods, but large differences for the *b* constant (the *Y* value when $x = 0$) were observed between the *GeNorm* method and classical method: -0.0092 vs. 0.46 (log2 ratio values). Therefore, *GeNorm* method adjusted much better to the microarray results as the *b* constant was closer to 0 in both tissues, so it was used to perform the analysis. The three most stable genes for hypothalamus were *Tbp, Ywhas*, and *Xpr1* (Supplementary Table S2).

SAM tests based on paired *t*-tests were performed to obtain a statistical significance of the differentially expressed genes. A 0.05 FDR threshold was used to consider genes significantly differentially expressed in the validation assay.

Quality Control

A correlation coefficient of 0.99 was obtained between ΔCt values from replicate values, giving high confidence to technical replicates (data not shown). Log2 ratios of genes determined to be differentially

[1] The online version of this article contains supplemental material.

expressed genes by microarray analysis were plotted against the log2 ratios obtained by TLDA analysis. A Pearson correlation coefficient of 0.65 ($P = 3.0 \times 10^{-13}$) comparing the two techniques was obtained.

Gene Ontology and Ingenuity Pathway Analysis

The confirmed genes validated from the microarray results, plus those ones confirmed among the literature-selected genes (<0.05 FDR) were used to generate networks, canonical pathways, and functions through the use of Ingenuity Pathways Analysis (IPA, Ingenuity Systems, www.ingenuity.com). A data set containing gene identifiers and corresponding expression values was uploaded into the application. Each gene identifier was mapped to its corresponding gene object in the Ingenuity Pathways Knowledge Base. A 0.001 FDR threshold cutoff was set to identify genes whose expression was significantly differentially regulated. These genes, called focus genes, were overlaid onto a global molecular network developed from information contained in the Ingenuity Pathways Knowledge Base. Networks of these focus genes were then algorithmically generated based on their connectivity.

RESULTS

To identify differentially expressed genes, we compared the hybridization signals of RNA transcripts obtained from hypothalamus from three male *anx/anx* mice vs. three male control mice. Since the phenotype is recessive, control mice included both animals heterozygous for the mutation or homozygous that do not carry the mutation. We confined our analysis to genes with a FDR of 0.001 (0.1%). With this stringent criterion, we aimed to identify the most reliably differentially expressed genes with a low risk of false positives, because our goal was to perform a posterior large qPCR replication experiment. Under this criterion, a total of 155 nonredundant genes were differentially expressed: 141 and 14, upregulated and downregulated, respectively (Supplemental Table S1).

To test the validity of the results of the transcriptome analysis, we designed a customized panel of low-density arrays, including TaqMan inventoried gene expression assays for our set of candidate genes. Target validation included 92 genes that were found deregulated in the array plus 87 additional assays from literature-candidate genes (Supplemental Table S2).

When normalizing by the three least variable genes in each tissue (see TaqMan data analysis section), the TaqMan results followed the same pattern in ~85% of the differentially expressed genes detected with Agilent microarrays, with 55% of them significant <0.05 FDR (Table 1, *top*; Table 2). The correlation between the microarray results and TLDA results was good (Pearson correlation = 0.65, $P < 10^{-13}$), even though in a proportion of cases the TaqMan and the Agilent probes were not mapping to the same exon of a given gene. Thus, among the 92 initially selected genes, 51 were confirmed as differentially expressed genes and considered as true positives (FDR <0.05, Table 1, *top*, Table 2). The vast majority of the TaqMan-tested genes were upregulated (mean fold change: 1.38) although seven genes were downregulated (mean fold: −1.67) (Tables 1 and 2; Fig. 1).

The confirmed genes validated from the microarray results plus those ones confirmed among the literature-selected genes (<0.05 FDR) were used to generate networks, canonical pathways, and functions through the use of IPA (www.ingenuity.com). According to our qRT-PCR results, when all the genes that appeared to be differentially expressed in hypothalamus were loaded to perform a core IPA analysis, the most significantly enriched network was cell death, cell morphology, and cancer ($P = 10^{-28}$). This network centers on tumor necrosis factor (TNF) and is involved in the regulation of a wide variety of biological processes related to acute phase response signaling, including cell proliferation, differentiation, apoptosis, lipid metabolism, and coagulation. Thirteen out of the 35 genes that defined the network were differentially expressed in *anx/anx* hypothalamus (Fig. 2, Table 2).

Table 1. *Validation of genes by TaqMan low-density arrays*

	Diff. Expr. Genes FDR <0.001 Agilent Arrays		
	Genes Tested by TaqMan	Confirmed by TaqMan (%)	Significant by TaqMan SAM < 0.05 FDR (%)
Upregulated	81	68 (84)	44 (54)
Downregulated	11	10 (91)	7 (64)
Total	92	78 (85)	51 (55)

Literature-based Selected Genes

Total genes selected	Significant by TaqMan SAM <0.05 FDR (%)	
87	Upregulated	12 (13.8)
	Downregulated	17 (19.6)

Top: confirmation rate of selected differentially expressed genes with 0.001 false discovery rate (FDR) according to Agilent arrays. *Bottom*: real-time TaqMan quantification of literature-selected genes. SAM, significance analysis of microarrays.

When we looked for enriched metabolic and cell signaling pathways we found that two of the most significant ones were the peroxisome proliferator-activated receptor (PPAR) signaling and activation cascades. Interestingly, molecules contained in this pathway overexpressed in the *anx/anx* mouse were the coactivator 1α of the peroxisome proliferative-activated receptor-γ, (*Pparg1a*), nuclear receptor corepressor 1 (*Ncor*), and phospholipase C β1 (*Plcb*). These genes are specifically involved in fatty acid oxidation and degradation, lipid homeostasis, adipocyte differentiation, and glucose and insulin homeostasis. Other specific pathways were identified for the hypothalamus, although often the analysis assigned a given gene to more than one pathway and included the Huntington's disease path (with focus genes involved in neurodegeneration) and the estrogen receptor signaling.

We also used real-time PCR to check the expression profiles of a set of genes that did not reach our very stringent threshold for considering the genes to be differentially expressed (FDR = 0.001), but for which compelling evidence of their involvement of eating behavior has been demonstrated. Twenty-nine out of 87 were found deregulated by low-density array analysis (Table 3). In six cases, the deregulation was more than twofold: adrenergic receptor α2b *(Adra2b*; fold change = 3.6), γ-aminobutyric acid (*Gaba-a*) receptor, subunit alpha 4 (*Gabra4a*; fold change = 3.2), and the muscarinic cholinergic receptor 3 (*Chrm3*; fold change = −2.0), melanin-concentrating hormone receptor 1 (*Mc1r*; fold change = 3.4), melanin-concentrating hormone receptor 1 (*Mc2r*; fold change = 2.6), and neuropeptide Y receptor Y6 (*Npy6r*; fold change = 8.7). Other deregulated pathways in *anx/anx* mice when observing all literature-nominated genes were the adrenergic signaling (*Adra2a*, *Adra2b)*, melanocortin signaling *(Cart, Mc1r, Mc2r,*

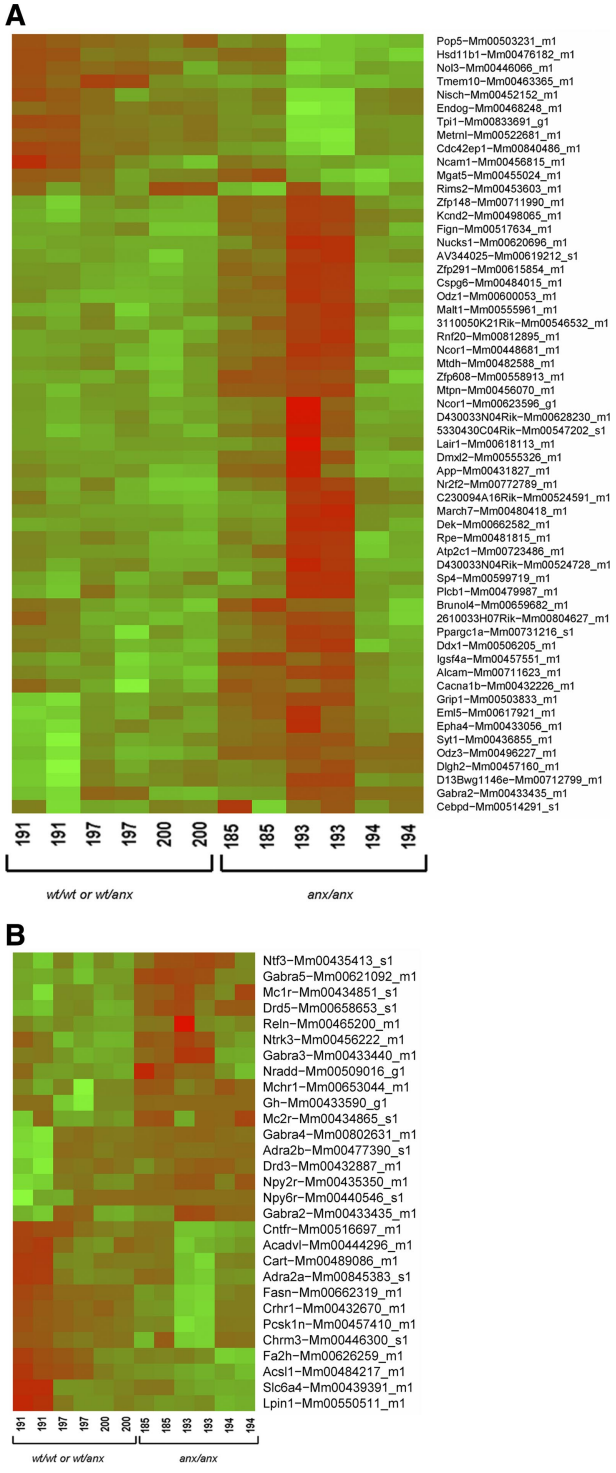

Fig. 1. Heat map of genes showing differential expression by real-time PCR using TaqMan low-density arrays. Only genes with a false discovery rate (FDR) <0.01 are shown. *A*: genes selected based on microarray results. *B*: genes selected based on literature search.

Npy2r, Npy6r, Mchr1, Pcsk1n, Pomc), neurotrophin signaling (Ntrk3, Ntf3, Cntfr, Nradd), GABA signaling (*Gabra2, Gabra3*, *Gabra4* and *Gabra5, Reln*), serotonin pathway (*Slc6a4*), dopamine signaling (*Drd3, Drd5*), and genes involved in hypothalamic fatty acid sensing (*Acadvl*, *Acsl1, Fa2h, Fasn*). In addition, several genes that when disrupted cause anorexia (*Crhr1, Chrm3*) or obesity (*Gh, Lpin*) were deregulated.

DISCUSSION

The aim of the present study was to identify differentially expressed genes in the hypothalamus of a widely accepted anorexia mouse model (*anx/anx*) using a microarray assay as a hypothesis-generating tool. We hypothesized that the expression profile may show in part deregulation of genes etiologically related to the anorexic phenotype, but also genes related to the prolonged food deprivation that mice were suffering, and thus a reflection of the compensatory responses in brain.

In the present work, initially, we determined the statistical significance using a very stringent FDR value to take into account correction for multiple testing and to reduce the number of false positives, since fold change alone does not address the reproducibility of the observed differences. Second, we used real-time RT-PCR through TLDA cards, which permitted us to perform 176 simultaneous real-time PCR reactions, therefore validating 85% of the statistically significant differentially expressed genes. This strategy allowed us to obtain valuable information from the entire set of microarray data and to have a broader insight into the global transcriptome of the *anx/anx* model. Despite fold changes being low, they were stable between replicates, which provided highly statistical *P* values. The biological relevance of genes that show small but highly significant changes in expression is of special interest in the study of the central nervous system (CNS), where subtle changes are often expected (56), and most of them were eventually proved to be truly differentially expressed from the qPCR validation experiments. In addition, we could detect differential expression of 29 out of the 87 genes selected based on literature search. Of the 29 candidate genes that were found to be differentially expressed by qPCR, 10 (34.5%) were differentially expressed in the microarray study when a 0.05 FDR threshold was set. Accordingly, these 10 genes appeared to be deregulated in the same direction by both methods, and for two of them, more than one probe was significantly deregulated in the array (two probes for *Adra2a* and three probes for *Gabra2*). Two possible reasons might explain why the remaining probes did not show differential expression. First, it is likely that the sensitivity is poorer in the microarray experiment compared with the TaqMan assays, which could detect a lower amount of RNA molecules and might have a greater range of detection. Another possibility is that, for certain genes, the isoforms targeted by the TaqMan assays might not be the same than those detected by the Agilent array.

The most significant network we identified, which was *cell death, cell morphology, and cancer*, contains 13 deregulated genes out of 35 focus genes contained in the network. This network centers on TNF, which is a proinflammatory cytokine known to induce anorexia and cachexia when a disconnection of anabolic pathways occurs and is typically upregulated in pathological processes, such as cancer, infection with human immunodeficiency virus or sepsis (22). Although TNF-α itself does not show differential expression according to the microarray results, it is possible that changes do not lie at the transcriptional level but at regulatory points not being measured by the microarray, such as translation, phosphorylation, cleavage,

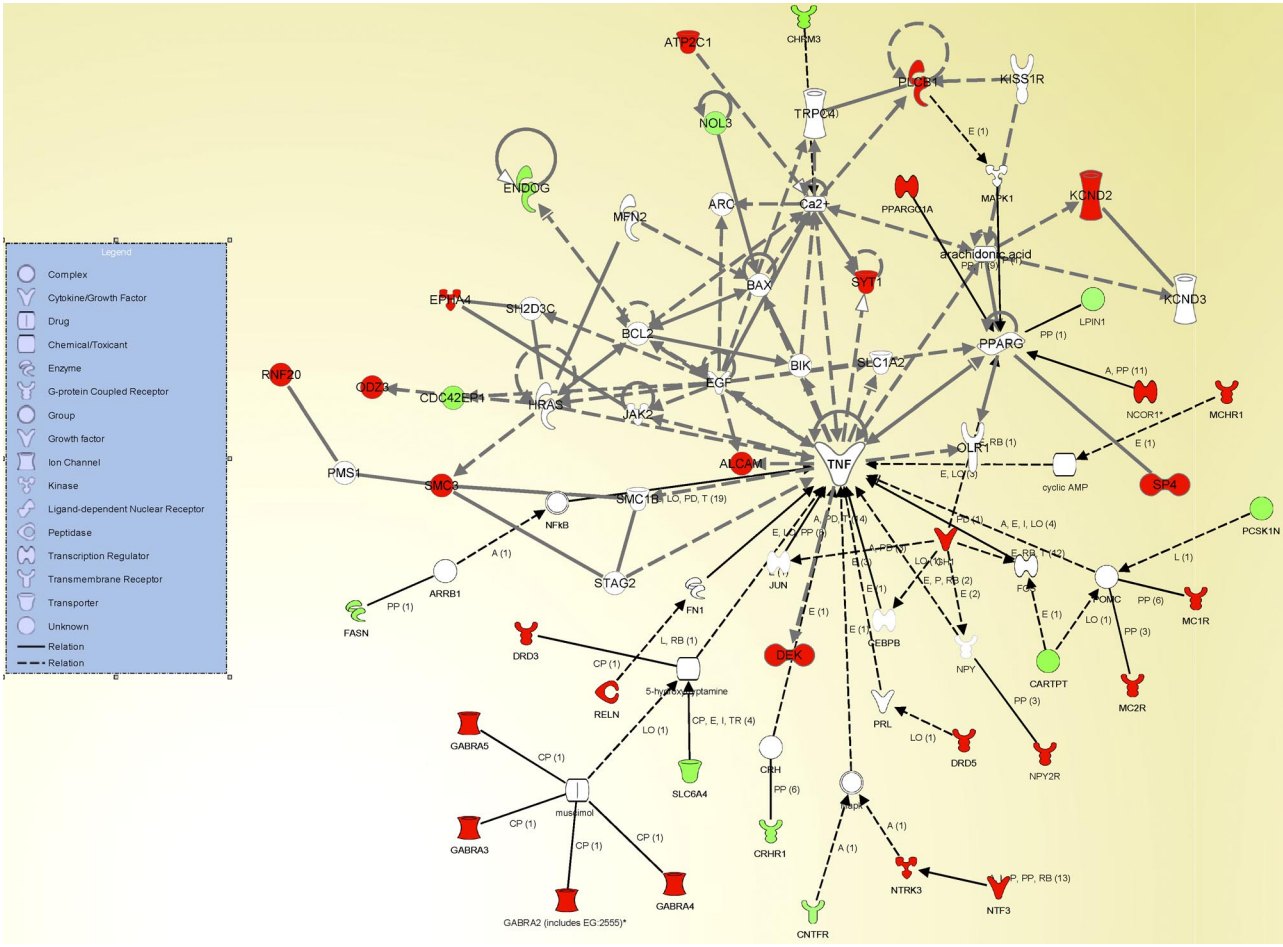

Fig. 2. Deregulated genes according to our TaqMan results were enriched in *cell death, cell morphology, and cancer* network genes. Upregulated genes are represented in red, downregulated in green. Genes related to body weight regulation that were selected from the literature and were deregulated in *anx/anx* were linked to this network through literature database search (black lines). ALCAM: activated leukocyte cell adhesion molecule; ARC: activity-regulated cytoskeleton-associated protein; ARRB1: arrestin, β1; ATP2C1: ATPase, Ca^{2+} transporting, type 2C, member 1; BAX: BCL2-associated X protein; BCL2: B-cell CLL/lymphoma 2; BIK: BCL2-interacting killer (apoptosis-inducing); CARTPT: CART prepropeptide; CDC42EP1: CDC42 effector protein (Rho GTPase binding) 1; CEBPB: CCAAT/enhancer binding protein (C/EBP)-β; CHRM3: cholinergic receptor, muscarinic 3; CNTFR: ciliary neurotrophic factor receptor; CRH: corticotropin releasing hormone; CRHR1: corticotropin releasing hormone receptor 1; DEK: DEK oncogene (DNA binding); DRD3: dopamine receptor D3; DRD5: dopamine receptor D5; EGF: epidermal growth factor (β-urogastrone); ENDOG: endonuclease G; EPHA4: EPH receptor A4; FASN: fatty acid synthase; FN1: fibronectin 1; FOS: v-fos FBJ murine osteosarcoma viral oncogene homolog; GABRA2 (includes EG:2555): γ-aminobutyric acid (GABA) A receptor, α2; GABRA3: γ-aminobutyric acid (GABA) A receptor, α3; GABRA4: γ-aminobutyric acid (GABA) A receptor, α4; GABRA5: γ-aminobutyric acid (GABA) A receptor, α5; GH1: growth hormone 1; HRAS: v-Ha-ras Harvey rat sarcoma viral oncogene homolog; JAK2: Janus kinase 2 (a protein tyrosine kinase); JUN: jun oncogene; KCND2: potassium voltage-gated channel, Shal-related subfamily, member 2; KCND3: potassium voltage-gated channel, Shal-related subfamily, member 3; KISS1R: KISS1 receptor; LPIN1: lipin 1; Mapk: MAP kinase, MAPK protein, NGF/EGF-dependent kinase; MAPK1: mitogen-activated protein kinase 1; MC1R: melanocortin 1 receptor (α-melanocyte stimulating hormone receptor); MC2R: melanocortin 2 receptor (adrenocorticotropic hormone); MCHR1: melanin-concentrating hormone receptor 1; MFN2: mitofusin 2; NCOR1: nuclear receptor co-repressor 1; NF-κB: nuclear factor-κB; NOL3: nucleolar protein 3 (apoptosis repressor with CARD domain); NPY: neuropeptide Y; NPY2R: neuropeptide Y receptor Y2; NTF3: neurotrophin 3; NTRK3: neurotrophic tyrosine kinase, receptor, type 3; ODZ3: odz, odd Oz/ten-m homolog 3 (*Drosophila*); OLR1: oxidized low-density lipoprotein (lectin-like) receptor 1; PCSK1N: proprotein convertase subtilisin/kexin type 1 inhibitor; PLCB1: phospholipase C β1 (phosphoinositide-specific); PMS1: PMS1 postmeiotic segregation increased 1 (*S. cerevisiae*); POMC: pro-opiomelanocortin (adrenocorticotropin/ β-lipotropin/α-melanocyte stimulating hormone/ β-melanocyte stimulating hormone/β-endorphin); PPARG: peroxisome proliferator-activated receptor-γ; PPARGC1A: peroxisome proliferator-activated receptor-γ, coactivator 1α; PRL: prolactin; RELN: reelin; RNF20: ring finger protein 20; SH2D3C: SH2 domain containing 3C; SLC1A2: solute carrier family 1 (glial high-affinity glutamate transporter), member 2; SLC6A4: solute carrier family 6 (neurotransmitter transporter, serotonin), member 4; SMC1B: structural maintenance of chromosomes 1B; SMC3: structural maintenance of chromosomes 3; SP4: Sp4 transcription factor; STAG2: stromal antigen 2; SYT1: synaptotagmin I; TNF: tumor necrosis factor (TNF superfamily, member 2); TRPC4: transient receptor potential cation channel, subfamily C, member 4.

modification, or degradation of the protein. However, a higher than expected number of genes either upregulated or downregulated in this particular pathway suggest a compensatory effect or a consequence of TNF-α activation. The genes that are differentially expressed in this network are discussed below. It is difficult to assess how the differences in the expression of TNF-α pathway genes lead to the activation or inactivation of this cascade, as some genes might be deregulated as a compensatory effect and others might be the cause of the alteration of the TNF-α pathway. However, the pathophysiology and neuroanatomical studies performed by Lachuer et al. (44) (see below) suggest that it is very plausible that an activation, rather than an inactivation, of the TNF-α cascade is present. Experimentally, it has been demonstrated that TNF-α

Table 2. *Significant differentially expressed genes selected according to Agilent arrays confirmed by TaqMan (SAM < 0.05 FDR)*

Gene Symbol	TaqMan Probe	Differentially Expressed Hypothalamus (significant probes, *n*)	TaqMan Fold Change HT	Gene Name
2610033H07Rik	Mm00804627_m1	UP (1)	1.16	RIKEN cDNA 2610033H07 gene
3110050K21Rik	Mm00546532_m1	UP (2)	1.21	RIKEN cDNA 3110050K21 gene
5330430C04Rik	Mm00547202_s1	UP (1)	1.72	RIKEN cDNA 5330430C04 gene
Alcam	Mm00711623_m1	UP (1)	1.34	activated leukocyte cell adhesion molecule
App	Mm00431827_m1	UP (1)	1.48	amyloid β (A4) precursor protein
Atp2c1	Mm00723486_m1	UP (2)	1.13	ATPase, Ca^{2+}-sequestering
AV344025	Mm00619212_s1	UP (1)	1.58	expressed sequence AV344025
Brunol4	Mm00659682_m1	UP (1)	1.19	bruno-like 4, RNA binding protein (*Drosophila*)
C230094A16Rik	Mm00524591_m1	UP (1)	1.3	RIKEN cDNA C230094A16 gene
Cacna1b	Mm00432226_m1	UP (1)	1.21	calcium channel, voltage-dependent, N type, α1B subunit
Cdc42ep1	Mm00840486_m1	DW (1)	−1.67	CDC42 effector protein (Rho GTPase binding) 1
Cspg6	Mm00484015_m1	UP (1)	1.58	chondroitin sulfate proteoglycan 6
D13Bwg1146e	Mm00712799_m1	UP (1)	1.35	DNA segment, Chr 13, Brigham & Womens Genetics 1146 expressed
D430033N04Rik	Mm00524728_m1	UP (1)	1.14	RIKEN cDNA D430033N04 gene
Ddx1	Mm00506205_m1	UP (1)	1.22	DEAD (Asp-Glu-Ala-Asp) box polypeptide 1
Dek	Mm00662582_m1	UP (1)	1.4	DEK oncogene (DNA binding)
Dlgh2	Mm00457160_m1	UP (1)	1.33	discs, large homolog 2 (*Drosophila*)
Dmxl2	Mm00555326_m1	UP (1)	1.48	Dmx-like 2
Eml5	Mm00617921_m1	UP (1)	1.61	echinoderm microtubule associated protein like 5
Endog	Mm00468248_m1	DW (1)	−1.72	endonuclease G
Epha4	Mm00433056_m1	UP (1)	1.99	Eph receptor A4
Fign	Mm00517634_m1	UP (1)	1.46	fidgetin
Gabra2	Mm00433435_m1	UP (2)	1.85	γ-aminobutyric acid (GABA-A) receptor, subunit α2
Grip1	Mm00503833_m1	UP (1)	1.53	glutamate receptor interacting protein 1
Hsd11b1*	Mm00476182_m1	DW (1)	−1.58	hydroxysteroid 11- β dehydrogenase 1
Igsf4a	Mm00457551_m1	UP (1)	1.27	immunoglobulin superfamily, member 4A
Kcnd2	Mm00498065_m1	UP (1)	1.49	potassium voltage-gated channel, Shal-related family, member 2
Lair1	Mm00618113_m1	UP (1)	1.35	leukocyte-associated Ig-like receptor 1
Malt1	Mm00555961_m1	UP (1)	1.51	mucosa-associated lymphoid tissue lymphoma translocation gene 1
March7	Mm00480418_m1	UP (1)	1.27	membrane-associated ring finger (C3HC4) 7
Metrnl	Mm00522681_m1	DW (1)	−1.85	meteorin, glial cell differentiation regulator-like
Mtdh	Mm00482588_m1	UP (1)	1.28	Metadherin
Mtpn	Mm00456070_m1	UP (1)	1.28	myotrophin
Ncor1*	Mm00448681_m1	UP (1)	1.22	nuclear receptor co-repressor 1
Ncor1*	Mm00623596_g1	UP (1)	1.42	nuclear receptor co-repressor 1
Nol3	Mm00446066_m1	DW (1)	−1.44	nucleolar protein 3 (apoptosis repressor with CARD domain)
Nr2f2	Mm00772789_m1	UP (1)	1.29	nuclear receptor subfamily 2, group F, member 2
Nucks1	Mm00620696_m1	UP (1)	1.3	nuclear casein kinase and cyclin-dependent kinase substrate 1
Odz1	Mm00600053_m1	UP (1)	1.51	odd Oz/ten-m homolog 1 (*Drosophila*)
Odz3	Mm00496227_m1	UP (1)	1.61	odd Oz/ten-m homolog 3 (*Drosophila*)
Plcb1*	Mm00479987_m1	UP (2)	1.22	phospholipase C, β1
Pop5	Mm00503231_m1	DW (1)	−1.78	processing of precursor 5, ribonuclease P/MRP family (S. cerevisiae)
Ppargc1a*	Mm00731216_s1	UP (1)	1.22	peroxisome proliferative activated receptor, γ, coactivator 1 α
Rnf20	Mm00812895_m1	UP (1)	1.38	ring finger protein 20
Rpe	Mm00481815_m1	UP (1)	1.18	ribulose-5-phosphate-3-epimerase
Sp4	Mm00599719_m1	UP (1)	1.2	trans-acting transcription factor 4
Syt1	Mm00436855_m1	UP (2)	1.56	synaptotagmin I
Tmem10	Mm00463365_m1	DW (1)	−1.66	transmembrane protein 10
Zfp148	Mm00711990_m1	UP (1)	1.49	zinc finger protein 148
Zfp291	Mm00615854_m1	UP (1)	1.38	zinc finger protein 291
Zfp608	Mm00558913_m1	UP (1)	1.38	zinc finger protein 608

*These genes have a role in body weight and eating behavior regulation: Hsd11b1, Orexigenic (50, 55); Ncor1, PPARG signaling (63); Plcb1, PPARG signaling (63); Ppargc1a, PPARG signaling (63).

induces anorexia by reducing the magnitude and duration of eating episodes (58). Moreover, its infusion is known to increase leptin secretion despite the decrease in food intake that would normally suppress leptin expression (24, 27, 61). Leptin levels are reduced in *anx/anx* mice (49), a fact that could be interpreted as a compensatory mechanism in response to decreased food intake. Moreover, cytokines are also able to induce robust anorexia even in the absence of leptin (7, 23), and low leptin levels have been reported in tumor-bearing rats (16) or in patients with cancer cachexia (10, 34, 66, 78).

Hence, taken together, these data suggest the activation of inflammatory cascades in *anx/anx* mice rather than a unique hypothalamic-derived anorexia phenotype. Our findings echo the results of Lachuer et al. (44), who found differential expression of several genes cytokines in *anx/anx* mice hypothalamus, and a recent neuropathological study that found activated microglia in several brain regions, supporting a CNS inflammation/neurodegeneration-associated process (54). Although the underlying mechanisms are unknown, glia can be activated after injury, releasing chemical mediators such as

Table 3. *Significant differentially expressed literature-based candidate genes as assessed by TaqMan (SAM < 0.05 FDR)*

Gene Symbol	TaqMan ID	TaqMan Fold Change (HT)	Gene Name	Reference No.
Adrenergic Receptors				
Adra2a	Mm00845383_s1	−1.35	adrenergic receptor, α2a	(59)
Adra2b	Mm00477390_s1	3.65	adrenergic receptor, α2b	(17)
Dopamine Signaling				
Drd3	Mm00432887_m1	1.98	dopamine receptor 3	(5, 25, 42, 43)
Drd5	Mm00658653_s1	1.37	dopamine receptor 5	(5, 25, 42, 43)
GABA signaling				
Gabra2	Mm00433435_m1	1.85	γ-aminobutyric acid (GABA-A) receptor, subunit α2	(8, 19, 60, 71, 74)
Gabra3	Mm00433440_m1	1.33	γ-aminobutyric acid (GABA-A) receptor, subunit α3	(8, 19, 60, 71, 74)
Gabra4	Mm00802631_m1	3.16	γ-aminobutyric acid (GABA-A) receptor, subunit α4	(8, 19, 60, 71, 74)
Gabra5	Mm00621092_m1	1.64	γ-aminobutyric acid (GABA-A) receptor, subunit α5	(8, 19, 60, 71, 74)
Reln	Mm00465200_m1	1.39	reelin	(8, 19, 60, 71, 74)
Hypothalamic fatty acid sensing				
Acadvl	Mm00444296_m1	−1.32	acyl-coenzyme A dehydrogenase, very long chain	(45)
Acsl1	Mm00484217_m1	−1.33	acyl-CoA synthetase long-chain family member 1	(45)
Fa2 h	Mm00626259_m1	−1.47	fatty acid 2-hydroxylase	(45)
Fasn	Mm00662319_m1	−1.57	fatty acid synthase	(29)
Anorexia knockout models				
Crhr1	Mm00432670_m1	−1.52	corticotropin releasing hormone receptor 1	(3)
Chrm3	Mm00446300_s1	−2.04	cholinergic receptor, muscarinic 3	(80)
Obesity knockout models				
Gh	Mm00433590_g1	>6*	growth hormone	(21)
Lpin1	Mm00550511_m1	−1.33	lipin 1	(57)
Melanocortin pathway				
Cart	Mm00489086_m1	−1.72	cocaine and amphetamine regulated transcript	(30, 77)
Mc1r	Mm00434851_s1	3.35	melanocortin 1 receptor	(64)
Mc2r	Mm00434865_s1	2.6	melanocortin 2 receptor	(64)
Mchr1	Mm00653044_m1	1.32	melanin-concentrating hormone receptor 1	(48)
Npy2r	Mm00435350_m1	1.72	neuropeptide Y receptor Y2	(4)
Npy6r	Mm00440546_s1	8.72	neuropeptide Y receptor Y6	(4)
Neurotrophin signaling				
Cntfr	Mm00516697_m1	−1.31	ciliary neurotrophic factor receptor	(47, 52, 79)
Nradd	Mm00509016_g1	1.2	neurotrophin receptor associated death domain	(11)
Ntf3	Mm00435413_s1	1.59	neurotrophin 3	(52)
Ntrk3	Mm00456222_m1	1.35	neurotrophic tyrosine kinase, receptor, type 3	(11)
Pcsk1n	Mm00457410_m1	−1.63	proprotein convertase subtilisin/kexin type 1 inhibitor	(52, 79)
Serotonin				
Slc6a4	Mm00439391_m1	−1.64	solute carrier family 6 (neurotransmitter transporter, serotonin), member 4	(38)

*Gh was detected in the three *anx/anx* animals but was undetectable in control mice. A precise fold change cannot be calculated.

CNS cytokines. These cytokines are able to modulate neuronal activity and synaptic strength through the release of hypothalamic histamine, serotonin, norepinephrine, and dopamine, all of them involved in the control of feeding (65, 67). We found low serotonin transporter (*Slc6a4*) levels in the hypothalamus that have also been reported in the Raphe nuclei of *anx/anx* mice (32), which could be the cause of the increased serotonin activity observed in this mouse model. In addition, reduced dopamine signaling but increased levels of dopamine synthesis genes have been described in *anx/anx* striatum (37). In our study, we observed an upregulation of *Drd3* and *Drd5* receptors, which could be a compensatory response to the reduced dopamine signaling. Finally, we found an intense upregulation of four GABA receptors, namely *Gabra2*, *Gabra3*, *Gabra4,* and *Gabra5*. The increase in the expression of these genes could reflect a compensatory effect, since activation of the TNF-α cascade causes an endocytosis of GABAA receptors, resulting in fewer surface receptors (72).

Lachuer et al. (44) found a downregulation of the NPY or AGRP mRNA genes in the *anx/anx* mice, thus confirming previous findings from other studies that also found altered levels of these two genes (13, 14, 33). Several data from our study also support a reduced responsiveness of the NPY circuitry in *anx/anx* mice. We found, for example, an upregulation of *Cck*, which inhibits orexigenic signals, or an increase in the expression of NPY receptors 2 and 6. Y2 receptors are abundant in the arcuate nucleus of the hypothalamus, and Y2 agonists inhibit NPY release from hypothalamic slices (40), which agrees with a strong inhibition of the NPY circuitry. Taken together, the expected compensatory effect of this pathway, which is usually induced by food deprivation, appears to be defective in the *anx/anx* mice, which might explain the persistent anorexia characteristic of this model.

Accordingly, the transcriptome profile of this model does not actually fit with the typical hypothalamic neuropeptide circuitry alteration in response to starvation but seems closer to an anorexia-cachexia syndrome like the classically observed in a cancer processes. Cachexia and starvation are the two major paradigms of malnutrition. Starvation is characterized by pure caloric deficiency. The organism responds with an increase in appetite, adapts metabolically to conserve lean mass and increase fat metabolism (15), changes that can be reversed by

appropriate feeding. In contrast, cachexia is associated with inflammatory or neoplasic conditions that evoke an acute-phase response, with diminished appetite concomitant with an increase in metabolic rate and a relative wasting of lean mass. In starvation, the positive energy balance is accomplished through the increased production, release, or action of NPY. During cachexia, the organism is maintained in a constant negative energy balance in which there is a persistent inhibition of the NPY orexigenic network, inducing anorexia and unopposed weight loss (31).

Some additional evidences from our results point toward the cachexia paradigm. We found, for instance, an upregulation of the PPAR activation pathway and signaling in *anx/anx* mice. Similar to other nuclear hormone receptors, PPARs act as ligand-activated transcription factors deeply involved in the maintenance of lipid and glucose homeostasis, by directly stimulating the transcription of genes involved in fatty acid oxidation (62).

In particular, the PPARγ signaling is activated by prostaglandins and leukotrienes, inflammatory mediators derived from the oxidative metabolism of arachidonic acid (20). On the other hand, the activator of the PPARγ (*Ppargc1a*, upregulated in the *anx/anx* mice) is able to activate uncoupling proteins, which stimulate thermogenesis in adipose tissue, elevating the resting energy expenditure and causing hypermetabolism, a cardinal feature of cachexia, but not of starvation (20, 41).

Intuitively one would believe that those genes known to induce appetite that are downregulated and those ones that are appetite suppressors that are upregulated are more likely to be responsible for the pathophysiology of this model and probably to contribute to the cachexia phenotype that these mice have. That is the case of melanocortin receptors 1 and 2 (*Mc1r* and *Mc2r*, respectively) or melanin-concentrating hormone receptor (*Mchr*), which although known to suppress feeding, are upregulated in anx/anx hypothalamus (48, 51, 53). Two other examples are the muscarinic receptor 3 (*Chrm3*) and fatty acid synthase (*Fasn*), which cause hypophagia and weight loss when disrupted (80), and are decreased in *anx/anx* hypothalamus. The reduction of Fasn, for instance, is a known mechanism of the repression of lipogenic factors that contributes to the impairment in the lipid-storing capacity of adipose tissue in cancer cachexia (10). Interestingly, *Gh* levels were detected in *anx/anx* mice but were undetectable in the three control mice, giving an approximate minimum fold-change of 16. Circulating Gh levels are pulsatile, with high peaks separated by valleys where the Gh is almost undetectable [reviewed in 1998 by Giustina and Veldhuis (26)]. Since dissection was performed in *anx/anx* mice and their respective controls at the same time, it is possible that this moment corresponded, for the control group, to a valley where the transcript was undetectable, while *anx/anx* mice had raised GH levels. This might be caused by enhanced catabolism and severe malnutrition, which causes growth arrest in juvenile animals and is associated with a condition referred to as acquired GH resistance, which can be defined by elevated circulating GH but decreased IGF-I levels. This is a common phenomenon seen in cancer-cachexia patients (9) that would perfectly fit with the model we are proposing, although we could not find any evidence for decreased mRNA levels of *Igf-1*. We also found results that may suggest a more complex anorexic profile, such a decrease of *Hsd11b1* and *Cart* expression, both of them anorexigenic, the later one shown to be reduced by in situ hybridization in arcuate nucleus and dorsomedial hypothalamic area of *anx/anx* mice (35). Moreover, we also found a decrease of *Cntfr*, which has been reported to cause a reduction in both NPY availability and the NPY-induced feeding response (79). These results might reflect the activation of pathways promoting food intake, which may be considered as compensatory to the cachectic state, even though their downstream effects may be countered by the activation of anorexigenic and catabolic pathways originating in different hypothalamic nuclei.

When the *anx/anx* mice were first described, they were found to have elevated levels of total blood urea nitrogen (BUN) and cholesterol (49). BUN is commonly used as a marker of protein intake, and in case of malnutrition is usually low, while higher levels reflect an increase in protein catabolism, a characteristic response of the acute-phase response in cachexia (31). On the other hand, increased lipid blood levels, specifically triglycerides and cholesterol, occur in cachexia but not starvation, reflecting an increase in adipocyte lipolysis that leads to fat mass loss (2).

In summary, our analysis shows that, at the transcriptome level, the *anx/anx* mice appear to have an increased systemic/CNS inflammatory response that, possibly through hypothalamus signaling, triggers a complex metabolic state comprising decreased appetite and significant weight loss. The data that we present not only open new insights on to the biological consequences of the undiscovered mutation that those mice harbor, but, surprisingly, it also turns out that the *anx/anx* mice might be a better anorexia-cachexia syndrome than a starvation model, as initially stated.

Although the stronger predictor of outcome is the severity of the underlying disease, the central objective of the prevention and treatment of the cachexia syndrome is to improve the life quality of the patient. It is thus probable that the *anx/anx* mice can be used as a cachexia animal model to understand the physiopathological alterations mediating this complex disease-accompanying condition and to test nutritional or pharmacological therapies.

ACKNOWLEDGMENTS

We thank Anna Wald for critically reading the manuscript, David Otero for performing the hybridizations, Stefanie Plaza and Roger Anglada for technical assistance with TLDA, and Moisès Burset for helpful suggestions to analyze Real-Time PCR data. We thank Anna Wald for critically reading the manuscript. Eulàlia Martí is also acknowledged for thorough revision of a final version of the manuscript. Finally, we acknowledge the three anonymous reviewers for constructive suggestions, which led to improvement of the manuscript.

The expression data reported in this paper have been deposited in the GEO (http://www.ncbi.nlm.nih.gov/geo) database (series GSE11426).

GRANTS

Financial support was received from the Ministry of Education and Science (SAF2005-01005, SAF2007-60827; and GEN2003-20651-C06-03), the "Fondo de Investigaciones Sanitarias de la Seguridad Social, FIS" (PI040632; PI040619); the Department of Health ("Generalitat de Catalunya"); and the Department of Universities, Research and Information Society (2005SGR00008, 2005SGR 00322) ("Generalitat de Catalunya"). J. M. Mercader was supported by the CRG under project SAF2002-00799 (Spanish Ministry of Science and Education) and by a Danone Institute fellowship. We are also grateful for support from Genome Spain to the National Genotyping Center (CeGen). This work was funded by two grants from the Spanish Ministry for Science and Technology SAF2003-05266 and SAF2004-06976 to L. Sumoy. L. Sumoy has singular research team recognition SGR2005-00404 by the Generalitat de Catalunya.

REFERENCES

1. **Adams KF, Schatzkin A, Harris TB, Kipnis V, Mouw T, Ballard-Barbash R, Hollenbeck A, Leitzmann MF.** Overweight, obesity, and mortality in a large prospective cohort of persons 50 to 71 years old. *N Engl J Med* 355: 763–778, 2006.
2. **Argiles JM, Alvarez B, Lopez-Soriano FJ.** The metabolic basis of cancer cachexia. *Med Res Rev* 17: 477–498, 1997.
3. **Bale TL, Contarino A, Smith GW, Chan R, Gold LH, Sawchenko PE, Koob GF, Vale WW, Lee KF.** Mice deficient for corticotropin-releasing hormone receptor-2 display anxiety-like behaviour and are hypersensitive to stress. *Nat Genet* 24: 410–414, 2000.
4. **Beck B.** Neuropeptide Y in normal eating and in genetic and dietary-induced obesity. *Philos Trans R Soc Lond B Biol Sci* 361: 1159–1185, 2006.
5. **Bergen AW, Yeager M, Welch RA, Haque K, Ganjei JK, van den Bree MB, Mazzanti C, Nardi I, Fichter MM, Halmi KA, Kaplan AS, Strober M, Treasure J, Woodside DB, Bulik CM, Bacanu SA, Devlin B, Berrettini WH, Goldman D, Kaye WH.** Association of multiple DRD2 polymorphisms with anorexia nervosa. *Neuropsychopharmacology* 30: 1703–1710, 2005.
6. **Berkman ND, Lohr KN, Bulik CM.** Outcomes of eating disorders: a systematic review of the literature. *Int J Eat Disord* 40: 293–309, 2007.
7. **Bessesen DH, Faggioni R.** Recently identified peptides involved in the regulation of body weight. *Semin Oncol* 25: 28–32, 1998.
8. **Beverly JL, Martin RJ.** Increased GABA shunt activity in VMN of three hyperphagic rat models. *Am J Physiol Regul Integr Comp Physiol* 256: R1225–R1231, 1989.
9. **Bing C.** Insight into the growth hormone-insulin-like growth factor-I axis in cancer cachexia. *Br J Nutr* 93: 761–763, 2005.
10. **Bing C, Russell S, Becket E, Pope M, Tisdale MJ, Trayhurn P, Jenkins JR.** Adipose atrophy in cancer cachexia: morphologic and molecular analysis of adipose tissue in tumour-bearing mice. *Br J Cancer* 95: 1028–1037, 2006.
11. **Bray MS, Boerwinkle E, Hanis CL.** Sequence variation within the neuropeptide Y gene and obesity in Mexican Americans. *Obes Res* 8: 219–226, 2000.
12. **Broberger C, Johansen J, Brismar H, Johansson C, Schalling M, Hokfelt T.** Changes in neuropeptide Y receptors and pro-opiomelanocortin in the anorexia (anx/anx) mouse hypothalamus. *J Neurosci* 19: 7130–7139, 1999.
13. **Broberger C, Johansen J, Johansson C, Schalling M, Hokfelt T.** The neuropeptide Y/agouti gene-related protein (AGRP) brain circuitry in normal, anorectic, and monosodium glutamate-treated mice. *Proc Natl Acad Sci USA* 95: 15043–15048, 1998.
14. **Broberger C, Johansen J, Schalling M, Hokfelt T.** Hypothalamic neurohistochemistry of the murine anorexia (anx/anx) mutation: altered processing of neuropeptide Y in the arcuate nucleus. *J Comp Neurol* 387: 124–135, 1997.
15. **Cahill GF Jr.** Starvation in man. *N Engl J Med* 282: 668–675, 1970.
16. **Chance WT, Sheriff S, Moore J, Peng F, Balasubramaniam A.** Reciprocal changes in hypothalamic receptor binding and circulating leptin in anorectic tumor-bearing rats. *Brain Res* 803: 27–33, 1998.
17. **Cheng JT, Kuo DY.** Both alpha1-adrenergic and D(1)-dopaminergic neurotransmissions are involved in phenylpropanolamine-mediated feeding suppression in mice. *Neurosci Lett* 347: 136–138, 2003.
18. **Clapcote SJ, Roder JC.** Simplex PCR assay for sex determination in mice. *Biotechniques* 38: 702, 704, 706, 2005.
19. **Coscina DV, Nobrega JN.** Anorectic potency of inhibiting GABA transaminase in brain: studies of hypothalamic, dietary and genetic obesities. *Int J Obes* 8, *Suppl* 1: 191–200, 1984.
20. **Desvergne B, Wahli W.** Peroxisome proliferator-activated receptors: nuclear control of metabolism. *Endocr Rev* 20: 649–688, 1999.
21. **Donahue LR, Beamer WG.** Growth hormone deficiency in 'little' mice results in aberrant body composition, reduced insulin-like growth factor-I and insulin-like growth factor-binding protein-3 (IGFBP-3), but does not affect IGFBP-2, -1 or -4. *J Endocrinol* 136: 91–104, 1993.
22. **Esper DH, Harb WA.** The cancer cachexia syndrome: a review of metabolic and clinical manifestations. *Nutr Clin Pract* 20: 369–376, 2005.
23. **Faggioni R, Fuller J, Moser A, Feingold KR, Grunfeld C.** LPS-induced anorexia in leptin-deficient (ob/ob) and leptin receptor-deficient (db/db) mice. *Am J Physiol Regul Integr Comp Physiol* 273: R181–R186, 1997.
24. **Finck BN, Kelley KW, Dantzer R, Johnson RW.** In vivo and in vitro evidence for the involvement of tumor necrosis factor-alpha in the induction of leptin by lipopolysaccharide. *Endocrinology* 139: 2278–2283, 1998.
25. **Frank GK, Bailer UF, Henry SE, Drevets W, Meltzer CC, Price JC, Mathis CA, Wagner A, Hoge J, Ziolko S, Barbarich-Marsteller N, Weissfeld L, Kaye WH.** Increased dopamine D2/D3 receptor binding after recovery from anorexia nervosa measured by positron emission tomography and [11c]raclopride. *Biol Psychiatry* 58: 908–912, 2005.
26. **Giustina A, Veldhuis JD.** Pathophysiology of the neuroregulation of growth hormone secretion in experimental animals and the human. *Endocr Rev* 19: 717–797, 1998.
27. **Grunfeld C, Zhao C, Fuller J, Pollack A, Moser A, Friedman J, Feingold KR.** Endotoxin and cytokines induce expression of leptin, the ob gene product, in hamsters. *J Clin Invest* 97: 2152–2157, 1996.
28. **Hellemans J, Mortier G, De Paepe A, Speleman F, Vandesompele J.** qBase relative quantification framework and software for management and automated analysis of real-time quantitative PCR data. *Genome Biol* 8: R19, 2007.
29. **Hu Z, Cha SH, van Haasteren G, Wang J, Lane MD.** Effect of centrally administered C75, a fatty acid synthase inhibitor, on ghrelin secretion and its downstream effects. *Proc Natl Acad Sci USA* 102: 3972–3977, 2005.
30. **Hunter RG, Philpot K, Vicentic A, Dominguez G, Hubert GW, Kuhar MJ.** CART in feeding and obesity. *Trends Endocrinol Metab* 15: 454–459, 2004.
31. **Inui A.** Cancer anorexia-cachexia syndrome: current issues in research and management. *CA Cancer J Clin* 52: 72–91, 2002.
32. **Jahng JW, Houpt TA, Joh TH, Son JH.** Differential expression of monoamine oxidase A, serotonin transporter, tyrosine hydroxylase and norepinephrine transporter mRNA by anorexia mutation and food deprivation. *Brain Res Dev Brain Res* 107: 241–246, 1998.
33. **Jahng JW, Houpt TA, Kim SJ, Joh TH, Son JH.** Neuropeptide Y mRNA and serotonin innervation in the arcuate nucleus of anorexia mutant mice. *Brain Res* 790: 67–73, 1998.
34. **Jensen PB, Blume N, Mikkelsen JD, Larsen PJ, Jensen HI, Holst JJ, Madsen OD.** Transplantable rat glucagonomas cause acute onset of severe anorexia and adipsia despite highly elevated NPY mRNA levels in the hypothalamic arcuate nucleus. *J Clin Invest* 101: 503–510, 1998.
35. **Johansen JE, Broberger C, Lavebratt C, Johansson C, Kuhar MJ, Hokfelt T, Schalling M.** Hypothalamic CART and serum leptin levels are reduced in the anorectic (anx/anx) mouse. *Brain Res Mol Brain Res* 84: 97–105, 2000.
36. **Johansen JE, Fetissov S, Fischer H, Arvidsson S, Hokfelt T, Schalling M.** Approaches to anorexia in rodents: focus on the anx/anx mouse. *Eur J Pharmacol* 480: 171–176, 2003.
37. **Johansen JE, Teixeira VL, Johansson C, Serrao P, Berggren PO, Soares-Da-Silva P, Schalling M, Bertorello AM.** Altered dopaminergic transmission in the anorexic anx/anx mouse striatum. *Neuroreport* 12: 2737–2741, 2001.
38. **Kaye WH, Frank GK, Bailer UF, Henry SE, Meltzer CC, Price JC, Mathis CA, Wagner A.** Serotonin alterations in anorexia and bulimia nervosa: new insights from imaging studies. *Physiol Behav* 85: 73–81, 2005.
39. **Keski-Rahkonen A, Hoek HW, Susser ES, Linna MS, Sihvola E, Raevuori A, Bulik CM, Kaprio J, Rissanen A.** Epidemiology and course of anorexia nervosa in the community. *Am J Psychiatry* 164: 1259–1265, 2007.
40. **King PJ, Williams G, Doods H, Widdowson PS.** Effect of a selective neuropeptide Y Y(2) receptor antagonist, BIIE0246 on neuropeptide Y release. *Eur J Pharmacol* 396: R1–R3, 2000.
41. **Kotler DP.** Cachexia. *Ann Intern Med* 133: 622–634, 2000.
42. **Kuo DY.** Further evidence for the mediation of both subtypes of dopamine D1/D2 receptors and cerebral neuropeptide Y (NPY) in amphetamine-induced appetite suppression. *Behav Brain Res* 147: 149–155, 2003.
43. **Kuo DY.** Hypothalamic neuropeptide Y (NPY) and the attenuation of hyperphagia in streptozotocin diabetic rats treated with dopamine D1/D2 agonists. *Br J Pharmacol* 148: 640–647, 2006.
44. **Lachuer J, Ouyang L, Legras C, Del Rio J, Barlow C.** Gene expression profiling reveals an inflammatory process in the anx/anx mutant mice. *Brain Res Mol Brain Res* 139: 372–376, 2005.
45. **Lam TK, Schwartz GJ, Rossetti L.** Hypothalamic sensing of fatty acids. *Nat Neurosci* 8: 579–584, 2005.
46. **Lambert JF, Benoit BO, Colvin GA, Carlson J, Delville Y, Quesenberry PJ.** Quick sex determination of mouse fetuses. *J Neurosci Methods* 95: 127–132, 2000.

47. **Lambert PD, Anderson KD, Sleeman MW, Wong V, Tan J, Hijarunguru A, Corcoran TL, Murray JD, Thabet KE, Yancopoulos GD, Wiegand SJ.** Ciliary neurotrophic factor activates leptin-like pathways and reduces body fat, without cachexia or rebound weight gain, even in leptin-resistant obesity. *Proc Natl Acad Sci USA* 98: 4652–4657, 2001.
48. **Luthin DR.** Anti-obesity effects of small molecule melanin-concentrating hormone receptor 1 (MCHR1) antagonists. *Life Sci* 81: 423–440, 2007.
49. **Maltais LJ, Lane PW, Beamer WG.** Anorexia, a recessive mutation causing starvation in preweanling mice. *J Hered* 75: 468–472, 1984.
50. **Masuzaki H, Paterson J, Shinyama H, Morton NM, Mullins JJ, Seckl JR, Flier JS.** A transgenic model of visceral obesity and the metabolic syndrome. *Science* 294: 2166–2170, 2001.
51. **McQuade JA, Benoit SC, Xu M, Woods SC, Seeley RJ.** High-fat diet induced adiposity in mice with targeted disruption of the dopamine-3 receptor gene. *Behav Brain Res* 151: 313–319, 2004.
52. **Mercader JM, Ribases M, Gratacos M, Gonzalez JR, Bayes M, de Cid R, Badia A, Fernandez-Aranda F, Estivill X.** Altered brain-derived neurotrophic factor blood levels and gene variability are associated with anorexia and bulimia. *Genes Brain Behav* 6: 706–716, 2007.
53. **Millington GW.** The role of proopiomelanocortin (POMC) neurones in feeding behaviour. *Nutr Metab (Lond)* 4: 18, 2007.
54. **Nilsson I, Lindfors C, Fetissov SO, Hokfelt T, Johansen JE.** Aberrant agouti-related protein system in the hypothalamus of the anx/anx mouse is associated with activation of microglia. *J Comp Neurol* 507: 1128–1140, 2008.
55. **Paulmyer-Lacroix O, Boullu S, Oliver C, Alessi MC, Grino M.** Expression of the mRNA coding for 11beta-hydroxysteroid dehydrogenase type 1 in adipose tissue from obese patients: an in situ hybridization study. *J Clin Endocrinol Metab* 87: 2701–2705, 2002.
56. **Pavlidis P.** Using ANOVA for gene selection from microarray studies of the nervous system. *Methods* 31: 282–289, 2003.
57. **Phan J, Reue K.** Lipin, a lipodystrophy and obesity gene. *Cell Metab* 1: 73–83, 2005.
58. **Plata-Salaman CR.** Central nervous system mechanisms contributing to the cachexia-anorexia syndrome. *Nutrition* 16: 1009–1012, 2000.
59. **Polak J, Moro C, Klimcakova E, Hejnova J, Majercik M, Viguerie N, Langin D, Lafontan M, Stich V, Berlan M.** Dynamic strength training improves insulin sensitivity and functional balance between adrenergic alpha 2A and beta pathways in subcutaneous adipose tissue of obese subjects. *Diabetologia* 48: 2631–2640, 2005.
60. **Rosmond R, Bouchard C, Bjorntorp P.** Allelic variants in the GABA(A)alpha6 receptor subunit gene (GABRA6) is associated with abdominal obesity and cortisol secretion. *Int J Obes Relat Metab Disord* 26: 938–941, 2002.
61. **Sarraf P, Frederich RC, Turner EM, Ma G, Jaskowiak NT, Rivet DJ 3rd, Flier JS, Lowell BB, Fraker DL, Alexander HR.** Multiple cytokines and acute inflammation raise mouse leptin levels: potential role in inflammatory anorexia. *J Exp Med* 185: 171–175, 1997.
62. **Schoonjans K, Staels B, Auwerx J.** The peroxisome proliferator activated receptors (PPARS) and their effects on lipid metabolism and adipocyte differentiation. *Biochim Biophys Acta* 1302: 93–109, 1996.
63. **Schroeder-Gloeckler JM, Rahman SM, Janssen RC, Qiao L, Shao J, Roper M, Fischer SJ, Lowe E, Orlicky DJ, McManaman JL, Palmer C, Gitomer WL, Huang W, O'Doherty RM, Becker TC, Klemm DJ, Jensen DR, Pulawa LK, Eckel RH, Friedman JE.** CCAAT/enhancer-binding protein beta deletion reduces adiposity, hepatic steatosis, and diabetes in Lepr(db/db) mice. *J Biol Chem* 282: 15717–15729, 2007.
64. **Shimizu H, Inoue K, Mori M.** The leptin-dependent and -independent melanocortin signaling system: regulation of feeding and energy expenditure. *J Endocrinol* 193: 1–9, 2007.
65. **Shintani F, Kanba S, Nakaki T, Nibuya M, Kinoshita N, Suzuki E, Yagi G, Kato R, Asai M.** Interleukin-1 beta augments release of norepinephrine, dopamine, and serotonin in the rat anterior hypothalamus. *J Neurosci* 13: 3574–3581, 1993.
66. **Simons JP, Schols AM, Campfield LA, Wouters EF, Saris WH.** Plasma concentration of total leptin and human lung-cancer-associated cachexia. *Clin Sci (Lond)* 93: 273–277, 1997.
67. **Smagin GN, Swiergiel AH, Dunn AJ.** Peripheral administration of interleukin-1 increases extracellular concentrations of norepinephrine in rat hypothalamus: comparison with plasma corticosterone. *Psychoneuroendocrinology* 21: 83–93, 1996.
68. **Smyth GK.** Linear models and empirical bayes methods for assessing differential expression in microarray experiments. *Stat Appl Genet Mol Biol* 3: Article3, 2004.
69. **Solomon CG, Manson JE.** Obesity and mortality: a review of the epidemiologic data. *Am J Clin Nutr* 66: 1044S–1050S, 1997.
70. **Son JH, Baker H, Park DH, Joh TH.** Drastic and selective hyperinnervation of central serotonergic neurons in a lethal neurodevelopmental mouse mutant, Anorexia (anx). *Brain Res Mol Brain Res* 25: 129–134, 1994.
71. **Squadrito F, Sturniolo R, Arcadi F, Arcoraci V, Caputi AP.** Evidence that a GABAergic mechanism influences the development of obesity in obese Zucker rats. *Pharmacol Res Commun* 20: 1087–1088, 1988.
72. **Stellwagen D, Beattie EC, Seo JY, Malenka RC.** Differential regulation of AMPA receptor and GABA receptor trafficking by tumor necrosis factor-alpha. *J Neurosci* 25: 3219–3228, 2005.
73. **Tisdale MJ.** Cachexia in cancer patients. *Nat Rev Cancer* 2: 862–871, 2002.
74. **Tsujii S, Bray GA.** GABA-related feeding control in genetically obese rats. *Brain Res* 540: 48–54, 1991.
75. **Tusher VG, Tibshirani R, Chu G.** Significance analysis of microarrays applied to the ionizing radiation response. *Proc Natl Acad Sci USA* 98: 5116–5121, 2001.
76. **Vandesompele J, De Preter K, Pattyn F, Poppe B, Van Roy N, De Paepe A, Speleman F.** Accurate normalization of real-time quantitative RT-PCR data by geometric averaging of multiple internal control genes. *Genome Biol* 3: RESEARCH0034, 2002.
77. **Vicentic A, Jones DC.** The CART (cocaine- and amphetamine-regulated transcript) system in appetite and drug addiction. *J Pharmacol Exp Ther* 320: 499–506, 2007.
78. **Wallace AM, Sattar N, McMillan DC.** Effect of weight loss and the inflammatory response on leptin concentrations in gastrointestinal cancer patients. *Clin Cancer Res* 4: 2977–2979, 1998.
79. **Xu B, Dube MG, Kalra PS, Farmerie WG, Kaibara A, Moldawer LL, Martin D, Kalra SP.** Anorectic effects of the cytokine, ciliary neurotropic factor, are mediated by hypothalamic neuropeptide Y: comparison with leptin. *Endocrinology* 139: 466–473, 1998.
80. **Yamada M, Miyakawa T, Duttaroy A, Yamanaka A, Moriguchi T, Makita R, Ogawa M, Chou CJ, Xia B, Crawley JN, Felder CC, Deng CX, Wess J.** Mice lacking the M3 muscarinic acetylcholine receptor are hypophagic and lean. *Nature* 410: 207–212, 2001.